Proceeding *20th SEAGC - 3rd AGSSEA Conference in conjunction with 22nd Annual Indonesian National Conference on Geotechnical Engineering.* Jakarta - INDONESIA, 6 -7 November 2018. ISBN No. 978-602-17221-6-9

Investigation of Aqueous Phase Liquids Migration in Double-Porosity Soil under Isothermal and Non-Isothermal Effect

K.F. Loke[1], R. Nazir[2], and H. Moayedi[3]
[1,2,3] *Center of Tropical Geoengineering, Faculty of Civil Engineering, Universiti Teknologi Malaysia, 81310 Johor Bahru, Johor, Malaysia*
E-mail: [1]edwinloke84@yahoo.com; [2]ramlinazir@utm.my; and [3]hossein.moayedi@gmail.com

ABSTRACT: As in civil engineering field, the intricate problem emerges when subsurface system undergoes the vibration, isothermal and non-isothermal effect in double-porosity soil. This will influence the migration of aqueous phase liquid (APLs) in the subsurface system. A series of laboratory experimental were carried out to monitor and observe the characteristics of the soil structure and APLs migration in deformable double-porosity soil under vary temperature. In order to monitor the changes, a unique digital image processing technique was used. The contour pattern of APLs migration was plotted based on the generated Hue Saturation Intensity (HSI), image analysis using Matlab and Surfer software. The results of the experiments show that both samples do not have a uniform migration pattern. In addition, the migration of fluid in soil sample 2 (isothermal condition) was faster than sample 1 (non-isothermal condition). This is mainly because the condition of heat imposed into the soil could influence the duration required for the migration. It is found that the heat will slow down the speed of migration. It can be concluded that factors that significantly influence the APLs migration (under vibration, isothermal and non-isothermal effect) were the soil structure, soil fractured pattern, and soil temperature.
Keywords: Non-isothermal porous media, isothermal porous media, APLs migration, digital image analysis technique, geo-environmental.

1. INTRODUCTION

Both development and industrial projects have played a key part in contribution to climate changes, global warming, pollution and natural disaster, which led to negative impact on the health problem and geo-environment hazard. These problems have called attention to the vibration, non-isothermal and isothermal effect in double-porosity soil resulting influence the migration of APLs into groundwater resources. Therefore, the main problem that need to be focused is ensuring the geo-environment safety issues. Vibration could cause the soil structure rearrangement, soil structure unstable, cracked soil, and soil structure volumetric deformation, which could affect the characteristics of pore sizes in future (Loke et al., 2017). Double-porosity media was identified as a two specific sub-region scale with the soil condition of intra-aggregate and inter-aggregate pores, which can be found in both compacted soil and agriculture tops-soils (Li and Zhang, 2009). The structure of double-porosity soil affects the pattern and speed rate of liquids migration. Generally, the fractured porosity formations are characterized by the water-bearing formations. It is well established that the groundwater flows along fractured solid rocks. Indeed, the fractured solid rocks is the result of the break in the rock mass normally caused by tectonic force (Masciopinto et al., 2001). According to Krisnanto et al., (2014), the fractured soil plays an essential role in the liquids flow through the complicated soil structure.

The liquid migration included gravity infiltration and transport. It is influenced by factors such as moisture content and temperature (i.e. non-isothermal and isothermal condition) (Grifoll et al., 2005). Fredlund et al., (2010), recognized the mechanical properties and hydrological characteristics of the fractured soil could significantly change. Besides, the dual-continuum method is more reliable with fracture matrix compared to discrete-fractured model (Fredlund et al., 2010).

The image analysis method has been used in many research areas. This technique can be applied to investigate the liquid contaminants and determine the saturation rate of liquid (Luciano et al., 2010). The common ways to observe and monitor liquid migration in soils consisting many measuring apparatuses. This interfere with the sample original setup and not economic. The porosity and cracked soil are difficult to monitor by naked eyes, and for this reason, digital image processing was suitable and acceptable for use in this study. According to Ngien et al., (2012), the problem of very hard to gathering data concerning liquid migration characteristics and the physical experiments will go a long way in the effort to comprehensively monitor, observe, understand and evaluate the polluted liquid migration into the groundwater resources. Besides, a number of researchers such as Alazaiza et al., (2017) and Sitthiphat and Siam (2016), have conducted experiments on double-porosity soil, which have contributed to the knowledge. However, the studies were limited to common double-porosity soil and reaction such as vibration and non-isothermal effect was never imposed to the double-porosity soil.

Therefore, the main objective of this study was to apply the model concept of the soil that overlaps the three continuums of fracture porosity, intra-aggregate porosity and inter-aggregate porosity features as developed by Loke et al., (2018) with considering the condition of isothermal and non-isothermal. A series of laboratory experiment model were carried out to study the characteristics of APLs migration into a vibrated double-porosity soil. The experiments were conducted under the isothermal and non-isothermal condition by using digital image processing technique. Thus, this study aimed (i) to determine the characteristics of APLs migration in fractured double-porosity soil using digital image analysis, (ii) to distinguish the phenomena of APLs migration with the condition of isothermal and non-isothermal in fracture double-porosity soil and (iii) to identify the APLs migration speed rate for specific soil column circumference zone.

2. MATERIALS AND METHODS

2.1 Fracture Double-Porosity Soil Sample Preparation

To create a double-porosity characteristic conditions, the soil sample materials used in this study was a commercially available kaolin soil. The kaolin soil properties were tested based on BS 1377-2, (1990) and BS 1377-5, (1990) for the purpose of acquiring Atterberg limits, particles size distribution, soil particle density, and saturated permeability of the kaolin soil. The properties of kaolin soil sample are shown in Table 1.

Table 1 Kaolin soil properties

Property	Value
Liquid Limit (%)	41
Plastic Limit (%)	27.50
Plasticity Index (%)	13.50
Particle Density (Mg/M^3)	2.65
Sand: 2mm to 0.06mm (%)	3
Fine: Less than 0.06mm (%)	97
USCS Classification	Clay with low plasticity (CL)
Saturated Permeability (m/s)	5.42×10^{-9}

The method used to prepare the aggregated kaolin soil was based on the method developed by Bagherieh et al., 2009. As to prepare the soil sample specimens, the dried kaolin powder mixed with the water to make a 30% moisture content for the soil samples.

The dried kaolin powder was constantly poured into the distilled water to control the moisture content. The reason for chosen 30% moisture content for this study was because the optimum moisture content for the used kaolin soil was 28%. Next, as in the sample curing period, the moisture kaolin was kept in a cool condition for a minimum of 24 hours. In order to keep the moisture constant during the cooling the samples were placed in a re-sealable plastic bag. Thereafter, the cured mixtures were broken simply by hand and passed through a 2.36 mm sieve (sieve No. 8) to obtain kaolin granules to create the double-porosity soil structure. The kaolin granules were placed in an acrylic soil column and compressed to a height of 100 mm using a compression machine. The 100 mm height of soil sample was chosen to ensure uniformity through the sample depth. The prepared double-porosity kaolin soil sample is given in Figure 1.

Figure 1 The prepared double-porosity soil

An acrylic soil column with dimension of 150 mm high, 100 mm outer diameter and 94 mm inner diameter was used for the experiment. In order to induce the heat to the soil, two heater rods and 1 thermocouple rods were installed into the centre of the soil (Figure 2). The acrylic soil column with installed rods into the soil was perfectly fixed and bolted on the vibration table in order to prevent any movement of the soil column during vibration process. The setup of the vibration table to vibrate the double-porosity soil sample was developed by the author at the centre of geotropic in Universiti Teknologi Malaysia (UTM).

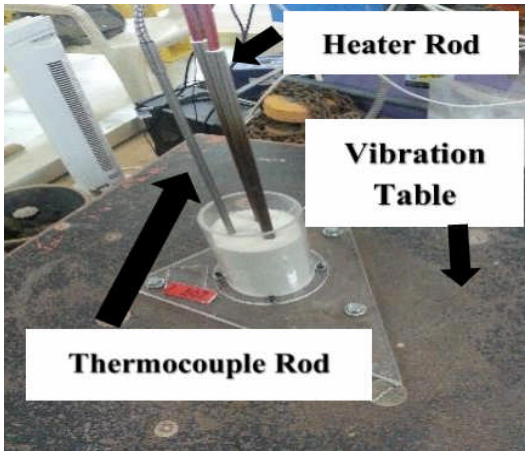

Figure 2: Heater and thermocouple setup

The vibration frequency for the vibration table was set on the control panel with 0.98 Hz frequency with 60 seconds duration for vibration process based on the previous literature. The result of fractured double-porosity soil sample with 30% moisture content after the vibration process is displayed in Figure 3. The concept of fracture double-porosity soil was to prove that the vibration effect had caused the double-porosity soil to fracture. The fractures on the top of soil sample can be clearly seen.

Figure 3 Soil sample after vibration process with fracture

2.2 Non-Isothermal Experiment Setup

The adjustable heater machine (for the purpose of the double-porosity soils) that is made in this study can impose heat to the whole volume of soil with the specific temperature. The invented adjustable heater machine design connected to two heater rods in order to induce and transfer the heat into the soil samples. As stated earlier one thermocouple rod was also used for the purpose of checking the actual initial soil temperature inside the tested soil. The cable of the rods was connected and fixed at the control panel on the heater machine. After connecting the cable to the heater machine, the heater induced the heat to the soil sample as in non-isothermal condition. However, in the isothermal condition only the samples were placed inside the room temperature and in these steps were carried out without using the adjustable heater machine. In each sample, the experimental measurement and setup of the V shape mirror and soil column position as well as the non-isothermal heater machine was arranged as shown in Figure 4 for APLs migration image acquisition.

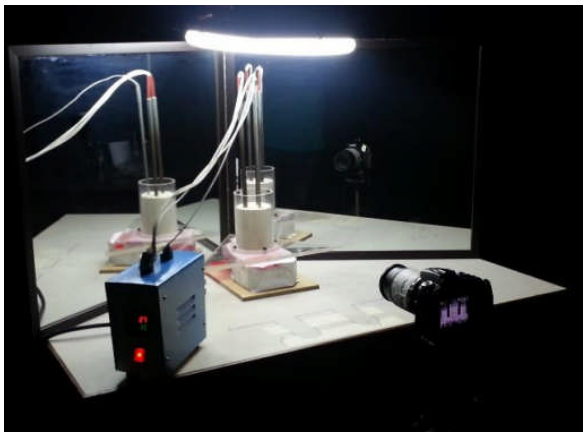

Figure 4 Digital image acquisition setup with non-isothermal heater machine

A Nikon D90 DSLR digital camera was used for APL migration image acquisition at specific time frequency interval. The setup of digital camera during the experiments was set at minimum shutter speed of 1/640 second and ISO speed set at ISO-2500, which has been implemented for all the soil sample experiments. To soften the problem of insufficient image acquisition, this experiment used a single digital camera, and two mirrors for reflection positioned behind the circular soil column were adjusted to enable a clear image facing the digital camera. Thus, the image of the APL migration throughout the whole area of soil column circumference can be initially captured by just a single click on the DSLR digital camera. The light source for soil sample come from linear fluorescent lamp-40 watt that was placed slightly above the circular soil column.

Both soil samples were first sheathed in white paper with pre-drawn gridline (20 mm x 20 mm) onto the soil column as a control point on the reference image. Once the reference image was taken, the pre-drawn gridline paper can be removed from the circular soil column. The adjustable heater machine starts to heat the soil with 30 Degrees Celsius and verified by the thermocouple to confirm the temperature of 30^{o} C for soil sample 1 with the non-isothermal condition. Meanwhile, sample 2 for isothermal condition was implemented in the room temperature of 23^{o} C without used the adjustable heater machine. Both experiments began by pouring the dyed water instantaneously onto the top centre of fractured aggregated soil sample in acrylic soil column. The quantity of 70 ml dyed water was used in samples 1 and 2. After the dyed water had covered the whole surface area of the fractured soil sample, the first digital image of aqueous phase liquid migration was taken. The dyed water migration pattern at a specific time frequency interval was captured for the rest of the subsequent digital images. A total of 115 images were subsequently recorded in 60 minutes for soil sample 1, while 118 images were captured in 90 minutes for soil sample 2.

2.3 Digital Image Processing Analysis Setup

The captured colour digital images were saved in JPEG format and transferred from Nikon D90 digital camera to computer for further image processing using Matlab routine and Surfer Software. A developed Matlab routine for digital image processing was used to extract the area of interest from captured image and to transform the area of interest from distorted image to a scale image via affine transformation method, which involves converting the JPEG scale images to Red Green Blue (RGB) and HSI images; extracting HSI digital value from HSI image and saving the HSI value in a text file using American Standard Code for Information Interchange (ASCII) format.

First, the surfer software was used to digitize the control point from reference image to extract actual image coordinates of control points to serve as control coordinate. While, area of interest refers to pre-determined migration boundary area (front image and V shape refection image) for sample 1 and 2 that contained the APL as shown in Figure 5. Matlab routine was then used to convert area of interest into RGB and HSI image format, where the values were extracted and saved in ASCII format. Matlab routine was used to loop three times for the subsequent digital image to extract and save the intensity values for all three section area of interest of the acrylic soil column. Finally, the contour plot pattern of the APL migration in fracture porous media based on the generated HSI value by digital image processing analysis was plotted. The HSI contour plot of APL migration behaviour in the condition of non-isothermal and isothermal condition can provide detailed information to facilitate researchers to understand the pattern of APL.

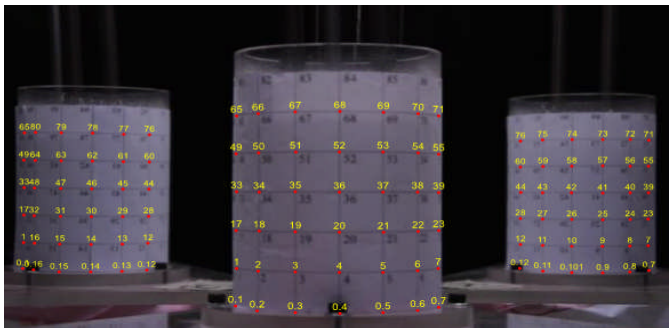

Figure 5 Digitization of the control point for area of interest

3. RESULTS AND DISCUSSION

After the APL migration process, the top view of the fractured soil samples 1 and 2 as shown in Figure 6. The actual size measurement for the column circumference zone was divided to aid visualize the crack position for samples 1 and 2.

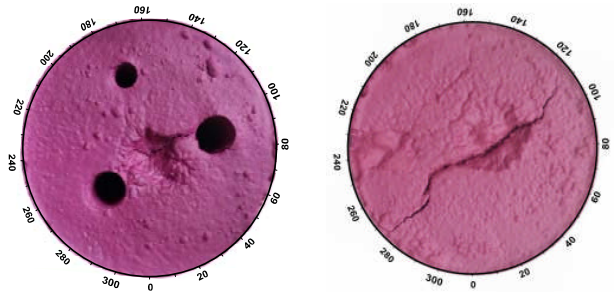

a) Soil sample 1 (Non-isothermal) b) Soil sample 2 (Isothermal)

Figure 6 APL migrated soil surface with measurement of actual column circumference zone for samples 1and 2

The downward migration pattern of HSI contour plot of APLs in fractured double-porosity soil sample with 30% moisture content for sample 1 (non-isothermal) and sample 2 (isothermal), respectively, are shown in Figures 7 and 8. The hole appear on sample 1 was the effect of the rods removed from the sample. When the HIS plot in curve joint the right and left boundary has formed the circular shape was clearly apparent in two-dimensional shape; however, the actual aqueous phase liquid migration in the acrylic soil column was one-dimensional.

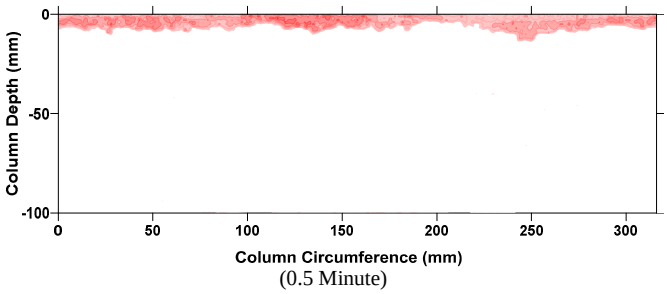

(0.5 Minute)

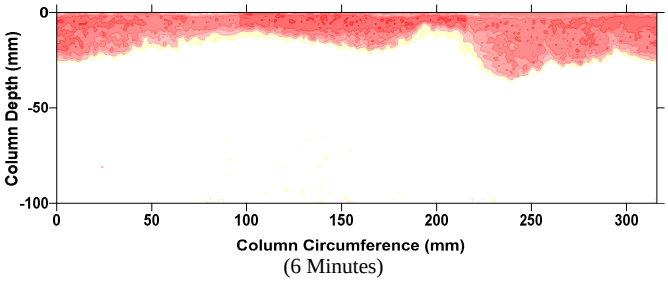

(6 Minutes)

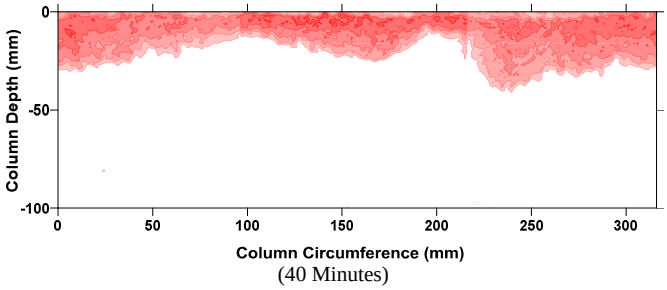

(40 Minutes)

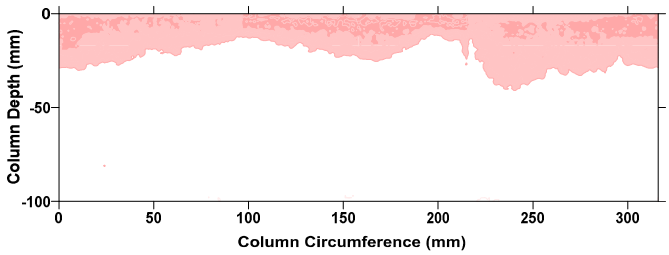

(90 Minutes)

Figure 7 HSI plots of downward migration in fractured double-porosity soil for non-isothermal condition

Both samples used 70 ml dyed distilled water was poured instantaneously on top of the soil samples surface by using glass funnel to ensure that the APL penetrated in one-dimension. In both experiments, the flow of the APL migration was not uniformly downward at the front boundary horizontal line due to the non-homogeneity of the fractured double-porosity soil structure. In soil sample 1, the selected HSI plots of dyed distilled water migration at intervals of 0.5, 6, 40, and 90 minutes, respectively, can been seen in Figure 7. Based on the observation and the HSI intensity contour plot results, the APL was not consistently downward the front x-axis horizontal line as the temperature and non-homogenous fractured affect the double-porosity soil sample. Further investigation, the faster migration occurred at the cracked soil surface condition compared to other locations on the soil surface that were not cracked in soil sample 1 as shown in Figure 6a. Monitor during migration process, the dyed water completely migrated on the whole top soil surface area into the heated fracture soil sample of the test, which took about 25 minutes. Meanwhile, the duration for dyed water migration from the top surface to the stop point was 90 minutes and further observation at 120 minutes indicated no further changes in migration pattern. 30 seconds after initiation of the experiment, the dyed water had penetrated just 10% of overall height of soil sample as shown in Figure 7. The deepest APL migration depth along the soil column was 38 mm out of 100 mm soil column at circumference length between 230 mm to 250 mm along the x-axis. The APL migration stopped at 90 minutes and did not fully migrate in this study because the water viscosity was higher compared to toluene viscosity (Assael et al., 2001). Thus, characteristics of water caused the high resistance and friction to gradual migration.

In soil sample 2, the interval of 0.5, 6, 20, and 60 minutes, respectively, was selected for dyed APL migration HSI plot as shown in Figure 8. The APL migration was similar to the result found in soil sample 1 in term of the APL migration no uniformly downward at the front boundary horizontal line. At 30 seconds after the initiation of the experiment, the dyed APL migration reached halfway of the test sample at the fractured location 90 mm to 140 mm along the column circumference length. For the dyed water to completely recede from view on the whole top soil surface area into the fractured soil sample of the test took about 20 minutes. Meanwhile, the overall duration for dyed APL migration from the top surface to the stop point was 60 minutes and further observation at 80 minutes showed no changes in migration pattern where the APL migration fully stopped where the dyed water migration between 60 to 190 mm along the x-axis have been reached approximately 85% downward depth of the soil column. The dyed water migrated fastest between 60 to 190 mm and 250 to 280 mm along the column circumference length. The deepest downward migration was 85 mm out of 100 mm of the soil sample height. The APL migration was not fully migrated because of the same condition like soil sample 1 due to the viscosity of the water have higher friction to gradual migration.

The phenomena of APL migration for non-isothermal and isothermal effect was difference because of the distinctive temperature. The non-isothermal soil sample took a longer time for the process of APL migration compared to the isothermal soil sample faster APL migration process. This could be because of the heat imposed in soil sample 1 has slow down the migration speed. Based on the observation soil sample 1, the soil condition was dried, and process of liquid evaporation occurred due to the heat induced in the soil sample. Both samples were not fully migrated due to water has higher viscosity compared to previous research by Sa'ari et al., (2015) was fully toluene migrated to the bottom of soil sample with the lower toluene viscosity. Besides, this could be because the physical bonding between toluene and soil weaker than water and soil. The physical bonding between toluene and soil was attributed to Van Der Waals Force, which are weaker than hydrogen bonding, which has stronger physical bonding between water and soil.

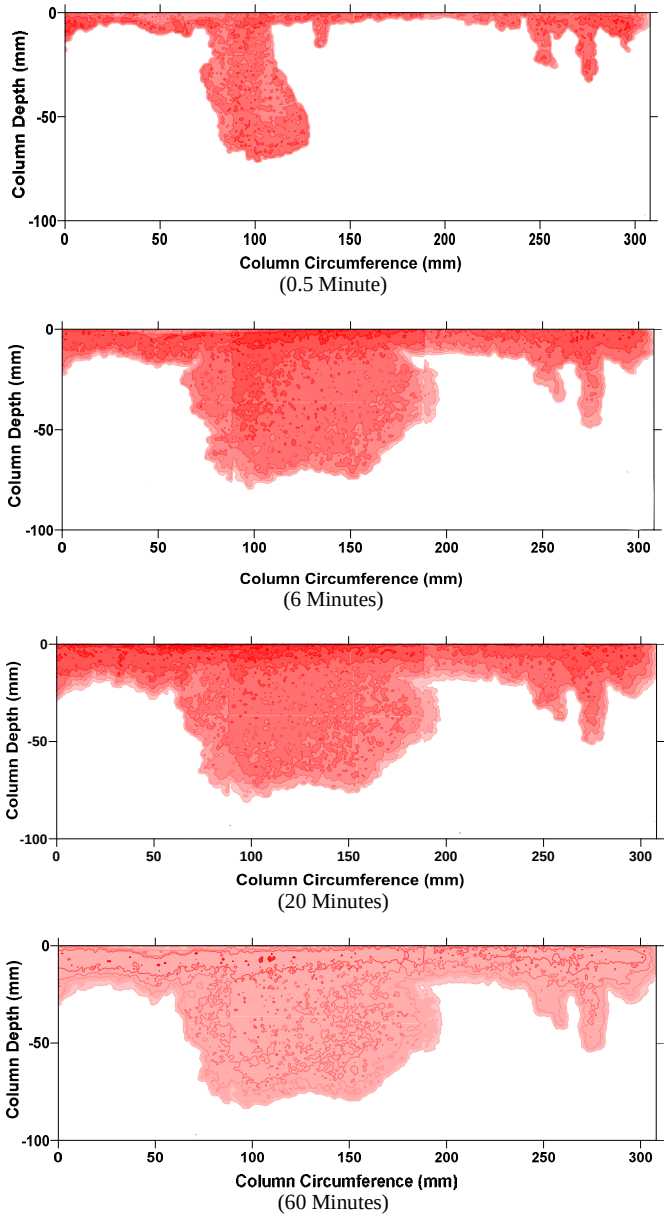

(0.5 Minute)
(6 Minutes)
(20 Minutes)
(60 Minutes)

Figure 8 HSI plots of downward migration in fractured double-porosity soil for isothermal condition

Figures 9 and 10 present the measured values of dyed water saturation depth as a function of time for every 30 mm column circumference in soil samples 1 and 2, respectively. Based on the result in Figure 9, it was found that the cumulative saturation depth of APL migration at 240 mm column circumference displayed the most critical migration downward within 30 seconds shown by the steepest gradient of the graph lines with that duration and continue to gradually incline horizontally until the end of the experiment. The second and third critical migration was at 270 mm and 0 mm column circumference, respectively. It within 6 minutes as shown by the sharp gradient of the graph lines within that duration and

continue after 6 minutes to gradually incline horizontally until the end of the experiment. Meanwhile, the rest of the column circumference positions continue a slow, decreased migration from start until the end of the experiment.

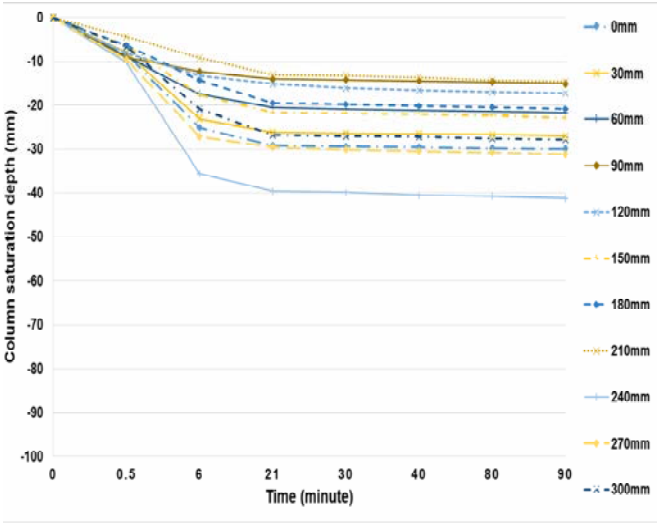

Figure 9 Measured values of dyed water saturation depth as a function of time for every 30 mm column circumference in sample 1

Based on Figure 10, the fastest and most critical migration downward to a cumulative saturation depth of APL migration occurred at 90 mm column circumference within 30 seconds as demonstrated by the steepest gradient of the graph lines within that duration, and after 30 seconds showed a gradual downward decline until the end of the experiment. 150 mm and 120 mm column circumference showed the second and third fastest critical penetration, respectively, within 60 seconds as demonstrated by the sharp gradient of the graph line within that duration and continue after 60 seconds to gradually incline horizontally until end of the experiment. Meanwhile, the remaining column circumference positions displayed slight decreased migration from start until the end of the experiment.

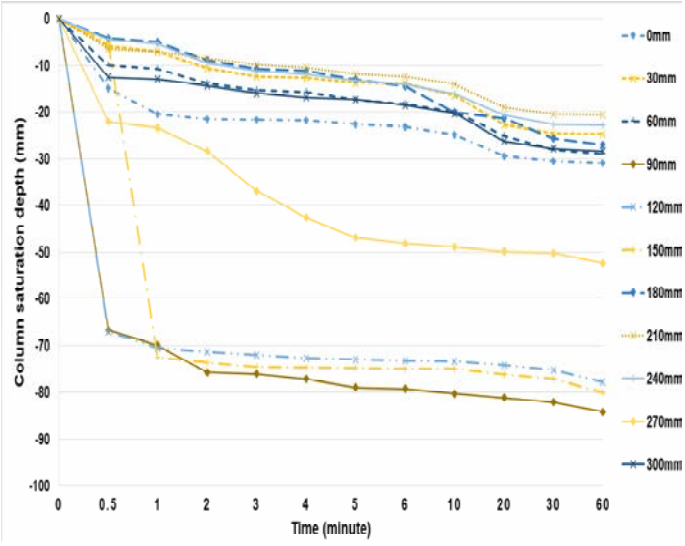

Figure 10 Measured values of dyed water saturation depth as a function of time for every 30 mm column circumference in sample 2

The calculated migration speed rate for the higher and overall average speed for every 30 mm column circumference zone was demonstrated in Table 2. Soil sample 1 shows the higher migration speed rate from initial to 30 seconds was at 240 mm column circumference zone with the speed rate of 0.339 mm/s. Meanwhile, the other high speed rates occurred at 270 mm and 0 mm column circumference with the value of 0.322 mm/s and 0.308 mm/s, respectively. Thus, the overall average dyed water migration speed rate for soil sample 1 is 0.043 mm/s. The highest average migration speed rate was at 240 mm column circumference zone at 0.061 mm/s. This could be because the larger fractured soil structure after the process of vibration was at the position of 240 mm.

The soil sample 2 displayed the higher migration speed rate from initial to 30 seconds at 90 mm column circumference zone with the speed rate of 2.234 mm/s. Meanwhile, the column circumference zone at 150 mm and 120 mm also have a high speed rate with the values of 2.231 mm/s and 2.224 mm/s, respectively. Therefore, the overall average dyed water migration speed rate for sample 2 is 0.097 mm/s. This scenario occurred because the soil sample 2 with isothermal condition without the temperature effect, could cause the penetration to be faster than soil sample 1.

Table 2 Migration speed rate for every 30 mm column circumference

Column Circumference Zone (mm)	Migration Flow Rate (mm/s)			
	Soil sample 1 (Non-Isothermal)		Soil sample 2 (Isothermal)	
	Higher Flow Between Initial to 30 Seconds	Average Flow for All the Time Interval	Higher Flow Between Initial to 30 Seconds	Average Flow for All the Time Interval
0	0.308	0.048	0.495	0.067
30	0.262	0.045	0.193	0.034
60	0.296	0.047	0.332	0.046
90	0.304	0.045	2.234	0.227
120	0.270	0.042	2.224	0.218
150	0.034	0.036	2.231	0.224
180	0.211	0.035	0.140	0.033
210	0.143	0.023	0.211	0.031
240	0.339	0.061	0.151	0.031
270	0.322	0.054	0.736	0.109
300	0.219	0.039	0.418	0.050

4. CONCLUSION

A series of physical laboratory experiment model on non-aqueous phase liquid migration, in fractured double-porosity soil, with 30% moisture content in the condition of isothermal and non-isothermal condition was conducted. This laboratory experiment was intentionally designed to investigate and differentiate the APL migration characteristic and pattern in the fractured double-porosity soil under the condition of different soil temperature. The digital image processing technique using Matlab routine and Surfer software was applied to analyse and extract the APL migration data acquired from captured digital image. From the results observed, both experiments indicated that in comparison to APL migration, the isothermal soil sample was migrated faster from the surface to the stopped point compared to the non-isothermal soil sample. The significant finding from this study was that the APL migration in non-isothermal soil sample undergoes the process of liquid evaporation and could dried the soil samples after the heat induce into the soil sample. Noteworthy, in both samples the APL migration was not fully migrated to the bottom of soil column. This is because the physical bonding between the soil and water attributed to Van Der Waals Force due to stronger hydrogen bonding.

The overall average of the fluid migration speed rates for experiment 1 and 2 were 0.043 mm/s and 0.097 mm/s, respectively, where the liquid migration speed rate was faster than 0.04 mm/s in the previous research by Sa'ari et al., (2015). This is because this study applied the effect of vibration on the double-porosity soil with the end product of fractured double-porosity soil. Therefore, it can be concluded that the factors that significantly influenced the APL migration in samples 1 and 2, respectively, was the structure of the

soil sample, fractured pattern of the soil sample, physical interaction between the liquid and soil sample, viscosity of liquid and the temperature of the soil sample. The HSI value and contour plot of dyed water migration could produce detailed particulars to professionals to understand and simulate the behaviour of APL migration that could be used to identify the remediation method most suitable to sustainable groundwater utilization.

5. ACKNOWLEDGEMENT

This study was supported by the Research Management Centre (RMC), Universiti Teknologi Malaysia under Research University Grant – Tier 1 (PY/2016/06547) from the Ministry of Higher Education Malaysia. The authors would also like to thank their respective University, Public Service Department Malaysia, Geotechnical Laboratory, Hydraulic and Hydrology Laboratory, Engineering Seismology and Earthquake Engineering Research Group (eSEER), and Survey Unit, Faculty of Civil Engineering, Universiti Teknologi Malaysia for kind assistance lent to this research. Special thanks to beloved late Professor Dr. Norhan Abd Rahman for his great contribution to this research, which has been passed away in 2018The first author was supported through the federal training award by the Public Service Department under Prime Minister's Department, Malaysia.

6. REFERENCES

Alazaiza, M.Y.D., Kong, S., Bob, M.M., Kamaruddin, S.A., Mohd, W. and Ishak, F. (2017) "Influence of Macro-pores on DNAPL Migration in Double-Porosity Soil Using Light Transmission Visualization Method", Transport in Porous Media, 117, Issues 1, pp103–123.

Assael, M.J., Avelino, H.M.T., Dalaouti, N.K., Fareleira, J.M.N.A. and Harris, K.R. (2001) "Reference correlation for the viscosity of liquid toluene from 213 to 373k at pressures to 250Mpa", International Journal of Thermophysics, 22, Issues 3, pp789–799.

Bagherieh, A.R., Khalili, N., Habibagahi, G. and Ghahramani, A. (2009) "Drying response and effective stress in a double porosity aggregated soil", Engineering Geology, 105, Issues 1-2, pp44–50.

British Standard Institute (BS 1377-2). (1990) Methods of test for soils for civil engineering purposes - Part 2: Classification Tests, 389 Chiswick High Road London W4 4AL, UK.

British Standard Institute (BS 1377-5). (1990) Methods of test for soils for civil engineering purposes - Part 5: Compressibility, permeability and durability test, 389 Chiswick High Road London W4 4AL, UK.

Fredlund, D.G., Houston, S.L., Nguyen, Q. and Fredlund, M.D. (2010) "Moisture Movement Through Cracked Clay Soil Profiles", Geotechnical and Geological Engineering, 28, Issues 6, pp865–888.

Grifoll, J., Gastó, J.M. and Cohen, Y. (2005) "Non-isothermal soil water transport and evaporation", Advances in Water Resources, 28, Issues 11, pp1254–1266.

Krisnanto, S., Rahardjo, H., Fredlund, D.G. and Leong, E.C. (2014) "Mapping of cracked soils and lateral water flow characteristics through a network of cracks", Engineering Geology, 172, pp12–25.

Li, X. and Zhang, L.M. (2009) "Characterization of dual-structure pore-size distribution of soil", Canadian Geotechnical Journal, 46, pp129–141.

Loke, K.F., Rahman, N.A. and Nazir, R. (2017) "Experimental study on unsaturated double- porosity soil phenomena under vibration effect", Jurnal Teknologi, 4, Issues 79, pp65–72.

Loke, K.F., Rahman, N.A., Nazir, R. and Lewis, R.W. (2018) "Study of aqueous amd non-aqueous phase liquid in fractured double-porosity soil using digital image processing", Geologia Croatica, 71, Issue 2, pp55–64.

Luciano, A., Viotti, P. and Papini, M.P. (2010) "Laboratory investigation of DNAPL migration in porous media", Journal of hazardous materials, 176, pp1006–1017.

Masciopinto, C., Benedini, M., Troisi, S. and Straface, S. (2001) Conceptual Models and Field Test Results in Porous and Fractured Media, In Groundwater Pollution Control, Southampton, UK: WIT Press.

Ngien, S.K., Rahman, N.A., Ahmad, K. and Lewis, R.W. (2012) "A review of experimental studies on double-porosity soils", Scientific Research and Essays, 7, issues 38, pp3243–3250.

Sa'ari, R., Rahman, N.A., Latif Abdul, N.H., Yusof, Z.M., Ngien, S.K., Kamaruddin, S.A., Mustaffar, M. and Hezmi, M.A. (2015) "Application of digital image processing technique in monitoring LNAPL migration in double porosity soil column". Jurnal Teknologi, 3(72), 23–29.

Sitthiphat, E. and Siam, Y. (2016) "Investigation of average optical density and degree of liquids saturation in sand by image analysis method", KKU Engineering Journal, 43, Issues SI, pp147–151.